Malaysian Journal of Mathematical Sciences 14(S) December : 171–184 (2020)
Special Issue: 2nd International Conference on Applied & Industrial Mathematics and Statistics 2019 (ICoAIMS 2019)

MALAYSIAN JOURNAL OF MATHEMATICAL SCIENCES

Journal homepage: http://einspem.upm.edu.my/journal

Modified Magnetic Field Flow of Casson Fluid and Solid Particles with Non-Linear Thermal Radiation Effect

Arifin, N. S.[1], Zokri, S. M.[2], Ariffin, N. A. S.[3], Kasim, A. R. M.*[4], and Salleh, M. Z.[4]

[1]*Faculty of Computer and Mathematical Sciences, Universiti Teknologi MARA (UiTM), Kampus Pasir Gudang, Malaysia*
[2]*Faculty of Computer and Mathematical Sciences, Universiti Teknologi MARA (UiTM), Kampus Kuala Terengganu, Malaysia*
[3]*Faculty of Computer and Mathematical Sciences, Universiti Teknologi MARA (UiTM), Kampus Jengka, Malaysia*
[4]*Centre for Mathematical Sciences, School of Computing & Applied Sciences, Universiti Malaysia Pahang, Malaysia*

E-mail: rahmanmohd@ump.edu.my
* *Corresponding author*

Received: 15 January 2020
Accepted: 12 November 2020

ABSTRACT

Two-phase flow problem has attracted considerable attention of many researchers due to its potential in investigating the flow characteristics of binary mixture of fluid and solid particles. In line with this, a mathematical model of convective flow of Casson fluid embedded with solid particles (dust) is formulated in order to study the interaction between the fluid phase and dust phase under the influences of non-linear thermal radiation and convective boundary condition (CBC) which is moving over a vertical stretching sheet. Through the use of similarity transformations, governing equations of fluid and dust phases are reduced into ordinary differential equations, which are then solved numerically by employing the Runge-Kutta Fehlberg (RKF45) method. The effects of radiation parameter and temperature ratio on velocity and temperature profiles, together with skin friction coefficient and Nusselt number are presented graphically as well as in tabular form. Findings reveal that, both effects improve the motion and temperature of fluid and dust phases, respectively.

Keywords: Fluid particle interaction, non-Newtonian, numerical solution, two-phase flow.

1. Introduction

The advancement in fluid mechanics has led to the development of innovative way in investigating the suspension of solid particles in fluid flow known as two-phase flow model, which describing the behavior of fluid-solid system. The industrial applications like transportation of petroleum, treatment of wastewater, emission of smoke from vehicles, piping of power plants and corrosive particles in mining generally involve the activities of fluid-solid movement, see Ramesh et al. (2017), where the interaction of these phases is significant. In conjunction with these implementations, a number of research activities in the respective flow can be found in the literature with various circumstances, for instance in numerous geometries, boundary conditions, and type of fluid based. Attia (2006) investigated the non-Newtonian Casson fluid flow embedded with solid particles over a circular pipe in the presence of Hall current impact. Meanwhile, in stretching sheet geometry, Arifin et al. (2017) explored the combined effect of aligned magnetic field and Newtonian heating by taking into account the dusty Casson fluid flow. Mahanthesh and Gireesha (2018) recently concerned with the Marangoni convective flow of Casson fluid pass a permeable plate under the influence of magnetic field with the addition of solid particles. Meanwhile, this study aims to continue the investigation on the flow behavior of dusty Casson fluid flow occupying a vertical stretching sheet associated with modified magnetic field and embedded with convective boundary condition (CBC) as heating state. Moreover, exploration in other flow models of dusty non-Newtonian fluid has gained considerable attention among researchers in various conditions, see Arifin et al. (2019), Kasim et al. (2019), Naramgari and Sulochana (2016) and Reddy et al. (2018).

The heat transport phenomenon of non-Newtonian fluid through radiation is one of the important elements arising in the boundary layer flow problems. In particular, radiation is the heat transfer within material in the form of electromagnetic waves, where it plays a pivotal role in determining the quality of final product in polymer industries. Many engineering practices involving the radiation instrument due to its involvement in such processes at high temperature, seeArchana et al. (2018). Therefore, several theoretical studies have been devoted to analyse the mechanism of thermal radiation of non-Newtonian fluid with dissimilar conditions, see Anwar et al. (2016), Aurangzaib et al. (2012), Mahanthesh et al. (2017), Zokri et al. (2018) and Sajid et al. (2018). However, these investigations are relevant only for the implementation of liner thermal radiation concept which account for small differences in temperature between wall and ambient. To overcome this limitation, nonlinear thermal radiation is introduced for fluid flow system involving high temperature difference. Sajid et al. (2018) and Khan et al. (2017) solved the fluid flow problem of Maxwell and Powel-Erying models, respectively in the presence of nanoparticles with nonlinear thermal radiation effect over a stretched surface. Another studies in flow problems associated with this particular impact for fluid-solid flow by observing the different fluid models have engaged the attention of some investigators, see Gireesha et al. (2016), Makinde et al. (2017), Ramesh et al. (2017) and Bhatti et al. (2016).

Motivated by the impactful researches as scrutinized above, this present study is dedicated to examine the two-phase boundary layer flow and thermal analysis of dusty Casson fluid past a vertical stretching sheet by focusing the non-linear thermal radiation effect. The modified magnetic field and mixed convection influences with CBC are also implanted in the investigation. Numerical solutions are obtained using Runge Kutta Fehlberg 45 (RKF45) method and expressed through graphs and tables.

2. Mathematical Models

Consider a steady, two-dimensional and incompressible of Casson fluid flow having dust particles over a vertical stretching sheet with the effects of nonlinear thermal radiation and aligned magnetic field under the thermal condition of CBC. The sheet is assumed to stretch in the $x-$direction and move with uniform velocity, $u_w(x)$, where $x-$axis is directed upward along the sheet, while$y-$axis is perpendicular to the surface of sheet. The geometric configuration of this study case is shown in Figure 1 . In addition, uniform magnetic field acting on the flow region is applied at any arbitrary angle $(0° - 90°)$ to the direction of fluid motion. The solid particles are presumed to be spherical in shape and uniform size where their density remains constant and the inter-particle collision may be neglected since they are considered to be diluted throughout the flow.

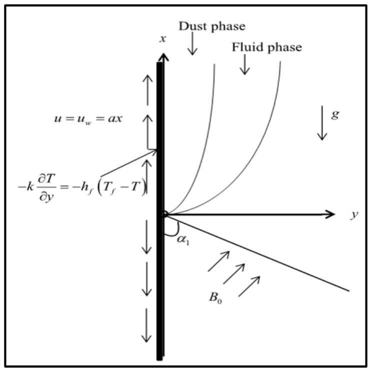

Figure 1: Physical model of two-phase flow

Summing up from the aforementioned assumptions and adopting the boundary layer approximation, the governing equations of dusty Casson fluid can be expressed in the Cartesian coordinate system as in Arifin et al. (2017) and Siddiqa et al. (2015).

Fluid phase:

$$\frac{\partial u}{\partial x} + \frac{\partial v}{\partial y} = 0 \tag{1}$$

$$\rho\left(u\frac{\partial u}{\partial x} + v\frac{\partial u}{\partial y}\right) = \mu_B\left(1 + \frac{1}{A}\right)\left(\frac{\partial^2 u}{\partial y^2}\right) + \frac{\rho_p}{\tau_v}(u_p - u) \\ - \sigma u {B_0}^2 \sin^2\alpha_1 + \rho g \beta^*(T - T_\infty) \tag{2}$$

$$\rho c_p\left(u\frac{\partial T}{\partial x} + v\frac{\partial T}{\partial y}\right) = k\left(\frac{\partial^2 T}{\partial y^2}\right) + \frac{\rho_p c_s}{\tau_T}(T_p - T) - \frac{\partial q_r}{\partial y}. \tag{3}$$

Dust phase:

$$\frac{\partial}{\partial x}(u_p) + \frac{\partial}{\partial y}(v_p) = 0 \tag{4}$$

$$\rho_p \left(u_p \frac{\partial u_p}{\partial x} + v_p \frac{\partial u_p}{\partial y} \right) = \frac{\rho_p}{\tau_v}(u - u_p) \tag{5}$$

$$\rho_p c_s \left(u_p \frac{\partial T_p}{\partial x} + v_p \frac{\partial T_p}{\partial y} \right) = -\frac{\rho_p c_s}{\tau_T}(T_p - T) \tag{6}$$

where (u, v), T, ρ, c_p, μ_B, σ, α_1, B_0 and q_r are the velocity components in (x, y) directions, temperature, density, specific heat at constant pressure, plastic dynamic viscosity of non-Newtonian, electrical conductivity, aligned angle, magnetic field and radiative heat flux for fluid phase, respectively. Meanwhile, (u_p, v_p), T_p, ρ_p, c_s, τ_v and τ_T denote the velocity components in (x, y) directions, temperature, density, specific heat, velocity and thermal relaxation time for dust phase, respectively.

For the case of non-linear thermal radiation, the Rosseland approximation is utilized to interpret for q_r in (3), which then can be simplified as Hayat et al. (2018).

$$q_r = -\frac{4\sigma^*}{3k^*}\frac{\partial T^4}{\partial y} = -\frac{16\sigma^*}{3k^*}T^3\frac{\partial T}{\partial y} \tag{7}$$

where σ^* and k^* signify to Stefan-Boltzmann constant and mean absorption coefficient, respectively. By using (7), energy equation (3) can be rewritten as

$$\rho c_p \left(u\frac{\partial T}{\partial x} + v\frac{\partial T}{\partial y} \right) = k\left(\frac{\partial^2 T}{\partial y^2} \right) + \frac{\rho_p c_s}{\tau_T}(T_p - T) + \frac{16\sigma^*}{3k^*}\frac{\partial}{\partial y}\left(T^3 \frac{\partial T}{\partial y} \right). \tag{8}$$

The present flow analysis is subjected to the following boundary conditions

$$
\begin{aligned}
&u = u_w(x) = ax,\ v = 0,\ \ -k\frac{\partial T}{\partial y} = -h_f(T_f - T) \text{ at } y = 0,\\
&u \to 0,\ u_p \to 0,\ v_p \to v,\ T \to T_\infty,\ T_p \to T_\infty \text{ as } y \to \infty
\end{aligned}
\tag{9}
$$

In (9), k, h_f, T_f and T_∞ correspond to the thermal conductivity, heat transfer coefficient, hot fluid temperature and ambient temperature. To obtain a set of similarity equation for the governing equations (1), (2), (4) to (6), (8) and (9) in the form of ordinary differential system, (10) is adopted, see Kumar et al. (2017).

$$
\begin{aligned}
&u = axf'(\eta),\ v = -(a\upsilon)^{1/2} f(\eta),\ \eta = \left(\frac{a}{\upsilon}\right)^{1/2} y,\ \theta(\eta) = \frac{T - T_\infty}{T_f - T_\infty},\\
&u_p = axF'(\eta),\ v_p = (a\upsilon)^{1/2} F(\eta),\ \theta_p(\eta) = \frac{T_p - T_\infty}{T_f - T_\infty}.
\end{aligned}
\tag{10}
$$

The resulting equations are obtained as follows.

$$
\begin{aligned}
&\left(1 + \frac{1}{A}\right) f'''(\eta) + f(\eta)f''(\eta) - (f'(\eta))^2 + \beta N\left(F'(\eta)\right.\\
&\left. - f'(\eta)\right) - M\sin^2\alpha_1 f'(\eta) + \lambda\theta(\eta) = 0
\end{aligned}
\tag{11}
$$

$$
\begin{aligned}
&\left[1 + \frac{4}{3}R(1 + (\theta_w - 1)\theta(\eta))^3\right]\theta''(\eta) + 4R(\theta_w - 1)\left(1 + (\theta_w - 1)\right.\\
&\left.\theta(\eta)\right)^2 (\theta'(\eta))^2 + \Pr f(\eta)\theta'(\eta) + \frac{2}{3}\beta N\left(\theta_p(\eta) - \theta(\eta)\right) = 0
\end{aligned}
\tag{12}
$$

$$
(F'(\eta))^2 - F(\eta)F''(\eta) + \beta\left(F'(\eta) - f'(\eta)\right) = 0 \tag{13}
$$

$$
{\theta_p}'(\eta)F(\eta) + \frac{2}{3}\frac{\beta}{\Pr\gamma}\left(\theta(\eta) - \theta_p(\eta)\right) = 0 \tag{14}
$$

together with the transformed boundary conditions as

$$\begin{aligned} &f(0)=0,\ f'(0)=1,\ \theta'(0)=-Bi\,(1-\theta(0))\ \text{ at } \eta=0 \\ &f'(\eta)\to 0,\ F(\eta)\to 0,\ F(\eta)\to f(\eta),\ \theta(\eta)\to 0,\ \theta_p(\eta)\to 0 \text{ as } \eta\to\infty. \end{aligned} \tag{15}$$

In (11) to (15), a notation prime (’) corresponds to the differentiation with respect to η. Additionally, several parameters of Casson parameter, A, mass concentration of particle phase, N, magnetic field parameter, M, fluid-particle interaction parameter, β, Prandtl number, Pr, specific heat ratio of mixture, γ, Biot number, Bi, temperature ratio parameter, θ_w, radiation parameter, R, mixed convection parameter, λ, Grashoff number, G_r and Reynold number, Re_x can be defined as

$$\begin{aligned} &A=\mu_B\frac{\sqrt{2\pi_c}}{\rho_y},\ N=\frac{\rho_p}{\rho},\ M=\frac{\sigma B_0^2}{\rho a},\ \beta=\frac{1}{a\tau_v},\ \ \mathrm{Pr}=\frac{\mu c_p}{k},\ \gamma=\frac{c_s}{c_p}, \\ &Bi=-\frac{h_f}{k}\left(\frac{\upsilon}{a}\right)^{1/2},\theta_w=\frac{T_f}{T_\infty},\ R=\frac{4\sigma^* {T_\infty}^3}{kk^*},\ \lambda=\frac{Gr_x}{{\mathrm{Re}_x}^2}, \\ &Gr_x=\frac{g\beta*T_\infty x^3}{\upsilon^2},\ \mathrm{Re}_x=\frac{u_w(x)x}{\upsilon}. \end{aligned} \tag{16}$$

Furthermore, a significant association between τ_T and τ_v can be represented by $\tau_T=(3/2\ )\gamma\tau_v\,\mathrm{Pr}$, which implies that τ_T is fully complying with the Stoke’s law. It is worth to note that, (11) to (15) will have the true similarity solutions if all considered parameters are constant. To accomplish this condition, only parameter λ that appears in (11) needs to be redefined since it is a function of variable x. By following the study reported by Makinde (2011), the thermal expansion coefficient, β^* can be assumed as

$$\beta^*=cx \tag{17}$$

where c is constant. It important to mention that, the exact solution for (11) with negligible influences of dust particles, magnetic field and buoyancy force can be obtained by using the following expression, see Mukhopadhyay (2013).

$$f(\eta)=\left(1+\frac{1}{A}\right)^{1/2}\left(1-\exp\left(-\frac{\eta}{(1+1/A)^{1/2}}\right)\right) \tag{18}$$

which leads to,

$$f''(\eta) = -\left(1+\frac{1}{A}\right)^{-1/2}\left(\exp\left(-\frac{\eta}{(1+1/A)^{1/2}}\right)\right). \tag{19}$$

Next, the physical quantities of skin friction coefficient and Nusselt number for this present mathematical model are given as (20), where it is in agreement with the one mentioned by Sajid et al. (2018).

$$\begin{aligned} C_f {\mathrm{Re}_x}^{1/2} &= \left(1+\frac{1}{A}\right) f''(0) \\ Nu_x {\mathrm{Re}_x}^{-1/2} &= \left[1+\frac{4}{3}R(1+(\theta_w-1)\theta(0))^3\right]\theta'(0). \end{aligned} \tag{20}$$

Accordingly, from (19) and (20), the exact equation for skin friction coefficient takes the form of

$$C_f {\mathrm{Re}_x}^{1/2} = -\left(1+\frac{1}{A}\right)\left(1+\frac{1}{A}\right)^{-1/2} \tag{21}$$

where $f''(0) = -\left(1+\frac{1}{A}\right)^{-1/2}$. Note that, to show the applicability of the numerical method used, it is necessary for the present results to be compared with the exact solution. Thus,(21) will be computed for the purpose of validating the present solutions.

3. Mathematical Procedure

The numerical solutions for this current investigation have been obtained by using RKF45 method where (11) to (15) are computed in the Maple software. It is well known that this method is undeniably one of suitable approaches for solving the two-phase flow problem on the basis of it has been widely applied in many previous and recent studies within this research area. By having the finite boundary layer thickness, $\eta_\infty = 8$, the boundary conditions of this study are fully satisfied by means of both velocity and temperature profiles attain the asymptotic behavior, as displayed in Figure 2 to Figure 5 .

4. Results & Discussion

In this section, numerical solutions obtained for the convective flow of dusty Casson fluid have been analyzed in details. This present paper will concentrate on the discussion on the solutions for various values of R and θ_w by assigning a set of fixed value of $\Pr = 10,\ A = 2,\ M = 1.5,\ \alpha_1 = \pi/6\ ,\ \lambda = 1,\ N = \beta = 0.5$ and $Bi = 0.6$. The computation of $C_f {\rm Re}_x{}^{1/2}$ for the assorted values of A with and without the presence of magnetic field has been performed in order to validate the numerical solutions acquired in this study. Therefore, a direct comparison between present results with the exact equation (21) and existing study reported by Nadeem et al. (2013), who solved Casson fluid flow over a porous linearly stretching sheet by using RKF45 method are therefore carried out. From table 1, an excellent agreement is achieved which indicates that the current model and its findings are acceptable.

Table 2 shows the variation of skin friction coefficient, $C_f {\rm Re}_x{}^{1/2}$ and Nusselt number, $Nu_x {\rm Re}_x{}^{-1/2}$ with regard to parameters of of R and θ_w, respectively. From the table, the similar influences of R and θ_w on the variation of magnitude value of $C_f {\rm Re}_x{}^{1/2}$ and $Nu_x {\rm Re}_x{}^{-1/2}$ have been observed. It is found that, both parameters improve the values of $Nu_x {\rm Re}_x{}^{-1/2}$, but the opposite trend is observed in the magnitude value of $C_f {\rm Re}_x{}^{1/2}$. This could be because of the reason that any increase in both parameters results in boosting the surface temperature and thus, the fluid temperature close to surface becomes higher. The rate of energy transport to the fluid also gets accelerated which turns to reduce the drag force between the fluid and surface.

Further, the analysis of parameters of R and θ_w on the velocity and temperature profiles of fluid and dust phases, respectively are depicted in Figure 2 to Figure 5 . From Figure 2 and Figure 3 , it can be observed that the velocity and temperature profiles of fluid and dust phases increases as the value of R increases, at which a constant value of $\theta_w = 1.3$ is considered. Physically, more heat energy is released to the fluid flow resulting from enhancing the effect of R which subsequently decreases the fluid viscosity and rises the temperature profile. In Figure 4 and Figure 5 , velocity and temperature profiles of both phases enhances for increasing value of θ_w when $R = 0.5$ is fixed. This is due to the escalating of hot fluid temperature, T_f at the surface.

Table 1: Comparison of $-C_f \mathrm{Re}_x{}^{1/2}$ for various values of M and A.

M	A	Exact equation (21)	Nadeem et al. (2013)	Present
0	∞	1.0000	1.0042	1.0005
	5	1.0954	1.0954	1.0954
	1	1.4142	1.4142	1.4142
10	∞	-	3.3165	3.3166
	5	-	3.6331	3.6332
	1	-	4.6904	4.6904

Table 2: Numerical results of $-C_f \mathrm{Re}_x{}^{1/2}$ and $Nu_x \mathrm{Re}_x{}^{-1/2}$ for various values of R and θ_w.

R	θ_w	$C_f \mathrm{Re}_x{}^{1/2}$	$Nu_x \mathrm{Re}_x{}^{-1/2}$
0.4	1.3	1.4513	0.7437
0.8		1.4277	1.0027
1.2		1.4051	1.2533
1.6		1.3834	1.4954
0.5	0.5	1.4583	0.6679
	1.0	1.4511	0.7464
	1.5	1.4407	0.8602
	2.0	1.4248	1.0343

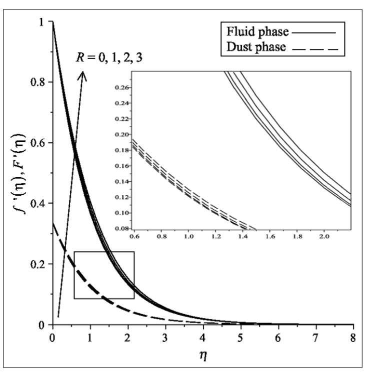

Figure 2: Variation of $f'(\eta)$ and $F'(\eta)$ for various values of R.

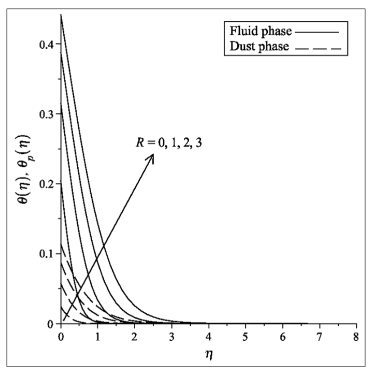

Figure 3: Variation of $\theta(\eta)$ and $\theta_p(\eta)$ for various values of R

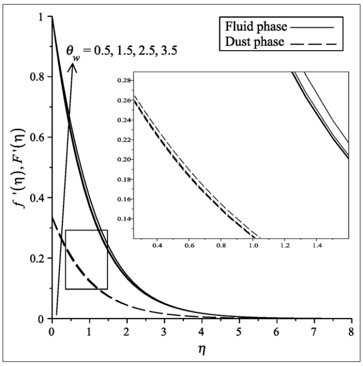

Figure 4: Variation of $f'(\eta)$ and $F'(\eta)$ for various values of θ_w.

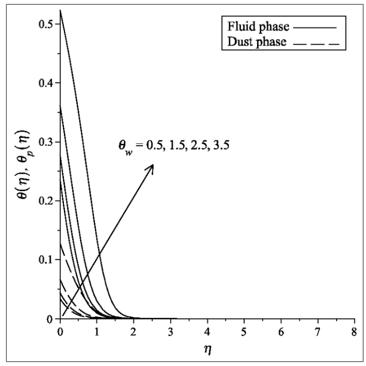

Figure 5: Variation of $\theta(\eta)$ and $\theta_p(\eta)$ for various values of θ_w.

5. Conclusion

This present investigation has reviewed the two-phase convective flow of dusty Casson fluid over a vertical stretching sheet by highlighting the effect of non-linear thermal radiation which involve the parameters of R and θ_w. From the mathematical analysis, a similar trend can be noticed in the motion and temperature distributions of fluid and dust phases, respectively when both parameters are increased. Nevertheless, the rising values of R and θ_w exhibits significant influence on temperature profile as compared to velocity profile. In the same manner, the Nusselt number is enhanced significantly when the values of $R$and θ_w changed, while the magnitude value of skin friction coefficient decreases gradually. The findings in this study are expected to contribute to better understanding of the characteristic of radiation in two-phase fluid flow as much as the solutions of single phase flow problems.

Acknowledgments

The authors gratefully acknowledge the financial support received from Universiti Malaysia Pahang for (RDU182307) and FRGS-RACER under RDU192602.

References

Anwar, M. I., Shafie, S., Kasim, A. R. M., and Salleh, M. Z. (2016). Radiation effect on mhd stagnation-point flow of a nanofluid over a nonlinear stretching sheet with convective boundary condition. *Heat Transfer Research*, 47(9):797–816.

Archana, M., Gireesha, B., Prasannakumara, B., and Gorla, R. (2018). Influence of nonlinear thermal radiation on rotating flow of casson nanofluid. *Nonlinear Engineering*, 7(2):91–101.

Arifin, N. S., Zokri, S. M., Kasim, A. R. M., Salleh, M. Z., and Mohammad, N. F. (2019). Two-phase mixed convection flow of dusty williamson fluid with aligned magnetic field over a vertical stretching sheet. In *Proceedings of the Third International Conference on Computing, Mathematics and Statistics (iCMS2017)*, pages 209–216.

Arifin, N. S., Zokri, S. M., Kasim, A. R. M., Salleh, M. Z., Yusoff, W. N. S. W., Mohammad, N. F., and Shafie, S. (2017). Aligned magnetic field on dusty casson fluid over a stretching sheet with newtonian heating. *Malaysian Journal of Fundamental and Applied Sciences*, 13(3):245–248.

Attia, H. A. (2006). Ion slip effect on the unsteady flow of a dusty casson fluid through a circular pipe. *Kragujevac Journal of Science*, 28:5–15.

Aurangzaib, K. A., Mohammad, N., and Shafie, S. (2012). Effect of thermal stratification on mhd free convection with heat and mass transfer over an unsteady stretching surface with heat source, hall current and chemical reaction. *International Journal of Advances in Engineering Sciences and Applied Mathematics*, 4(3):217–225.

Bhatti, M., Zeeshan, A., and Ellahi, R. (2016). Study of heat transfer with nonlinear thermal radiation on sinusoidal motion of magnetic solid particles in a dusty fluid. *Journal of Theoretical and Applied Mechanics*, 46(3):75–94.

Gireesha, B., Mahanthesh, B., Gorla, R. S. R., and Krupalakshmi, K. (2016). Mixed convection two-phase flow of maxwell fluid under the influence of non-linear thermal radiation, non-uniform heat source/sink and fluid-particle suspension. *Ain Shams Engineering Journal*, 9(4):735–746.

Hayat, T., Ullah, S., Khan, M. I., Alsaedi, A., and Zia, Q. Z. (2018). Non-darcy flow of water-based carbon nanotubes with nonlinear radiation and heat generation/absorption. *Results in Physics*, 8:473–480.

Kasim, A. R. M., Arifin, N. S., Zokri, S. M., and Salleh, M. Z. (2019). Fluid-particle interaction with buoyancy forces on jeffrey fluid with newtonian heating. *CFD Letters*, 11(1):1–16.

Khan, M., Irfan, M., Khan, W., and Ahmad, L. (2017). Modeling and simulation for 3d magneto eyring–powell nanomaterial subject to nonlinear thermal radiation and convective heating. *Results in Physics*, 7:1899–1906.

Kumar, K. G., Rudraswamy, N., Gireesha, B., and Manjunatha, S. (2017). Non linear thermal radiation effect on williamson fluid with particle-liquid suspension past a stretching surface. *Results in Physics*, 7:3196–3202.

Mahanthesh, B. and Gireesha, B. (2018). Scrutinization of thermal radiation, viscous dissipation and joule heating effects on marangoni convective two-phase flow of casson fluid with fluid-particle suspension. *Results in Physics*, 8:869–878.

Mahanthesh, B., Gireesha, B., Shehzad, S., Abbasi, F., and Gorla, R. (2017). Nonlinear three-dimensional stretched flow of an oldroyd-b fluid with convective condition, thermal radiation, and mixed convection. *Applied Mathematics and Mechanics*, 38(7):969–980.

Makinde, O. D. (2011). Similarity solution for natural convection from a moving vertical plate with internal heat generation and a convective boundary condition. *Thermal Science*, 15(1):137–143.

Makinde, O. D., Kumar, K. G., Manjunatha, S., and Gireesha, B. J. (2017). Effect of nonlinear thermal radiation on mhd boundary layer flow and melting heat transfer of micro-polar fluid over a stretching surface with fluid particles suspension. In *Defect and Diffusion Forum*, volume 378, pages 125–136.

Mukhopadhyay, S. (2013). Casson fluid flow and heat transfer over a nonlinearly stretching surface. *Chinese Physics B*, 22(7):074701.

Nadeem, S., Haq, R. U., Akbar, N. S., and Khan, Z. H. (2013). Mhd three-dimensional casson fluid flow past a porous linearly stretching sheet. *Alexandria Engineering Journal*, 52(4):577–582.

Naramgari, S. and Sulochana, C. (2016). Mhd flow of dusty nanofluid over a stretching surface with volume fraction of dust particles. *Ain Shams Engineering Journal*, 7(2):709–716.

Ramesh, G., Kumar, K. G., Shehzad, S., and Gireesha, B. (2017). Enhancement of radiation on hydromagnetic casson fluid flow towards a stretched cylinder with suspension of liquid-particles. *Canadian Journal of Physics*, 96(1):18–24.

Reddy, M. G., Rani, M. S., and Prasannakumara, C. (2018). Non-linear radiation and chemical reaction impacts on hydromagnetic particle suspension flow in non-newtonian fluids. *International Journal of Chemical Reactor Engineering*, 16(6):1–16.

Sajid, T., Sagheer, M., Hussain, S., and Bilal, M. (2018). Darcy-forchheimer flow of maxwell nanofluid flow with nonlinear thermal radiation and activation energy. *AIP Advances*, 8(3):035102. https://doi.org/10.1063/1.5019218.

Siddiqa, S., Hossain, M. A., and Saha, S. C. (2015). Two-phase natural convection flow of a dusty fluid. *International Journal of Numerical Methods for Heat & Fluid Flow*, 25(7):1542–1556.

Zokri, S. M., Arifin, N., Kasim, A. M., and Salleh, M. Z. (2018). Passive control of nanoparticles on mhd jeffrey nanofluid past a convectively heated moving plate with thermal radiation. *International Journal of Automotive and Mechanical Engineering*, 15(4):5775–5792.